Janusz PODLIŃSKI[1], Artur BERENDT[1], Anna NIEWULIS[1], Jerzy MIZERACZYK[1, 2]

The Szewalski Institute of Fluid Flow Machinery (1), Gdynia Maritime University (2)

Electrohydrodynamic secondary flow in the electrostatic precipitator with spiked electrodes

Abstract. *In this work, the results of electrohydrodynamic (EHD) secondary flow measurements in an electrostatic precipitator (ESP) with one-sided spike electrodes are presented. The EHD secondary flow was measured for one-sided spike electrodes with the spike tips directed either upstream or downstream the primary flow. The results showed different flow patterns for different spike tips direction in respect to the primary flow direction. This secondary flow patterns can have meaningful influence on the ESP collection efficiency.*

Streszczenie. *W niniejszej pracy zaprezentowano wyniki pomiarów przepływu elektrohydrodynamicznego w elektrofiltrze z elektrodami ostrzowymi z ostrzami po jednej stronie. Pomiary wykonano dla elektrod skierowanych ostrzami w górę oraz w dół przepływu pierwotnego. Uzyskane wyniki prezentują różne struktury przepływu w elektrofiltrze dla różnych położeń elektrod ostrzowych. Różne struktury przepływu mogą powodować znaczne różnice w skuteczności odpylania elektrofiltru.* ***(Wtórny przepływ elektrodynamiczny w elektrofiltrze z elektrodami osłonowymi)***

Keywords: electrostatic precipitator, electrohydrodynamic flow, Particle Image Velocimetry method.
Słowa kluczowe: elektrofiltr, przepływ elektrohydrodynamiczny, metoda Particle Image Velocimetry.

Introduction

Electrostatic precipitators (ESPs) are widely used as dust particle collectors. They are characterized by a high total particle collection efficiency (up to 99.9%) with a low pressure drop. However, the collection efficiency of submicron dust particles is much lower [1-4]. Submicron dust particles, which can contain traces of toxic elements, float relatively long in the atmosphere and can easily penetrate into human respiratory system. Therefore, in Europe new standards for emission of fine particles (PM2.5) has been introduced by the European Parliament [5]. The existing ESPs have to be modified to meet those new standards.

One of the proposal to improve the collection efficiency of submicron particles in ESPs was to use spike discharge electrodes. Typically, electrodes with spike tips on two sides of the discharge electrode are used. However, our results of electrohydrodynamic (EHD) secondary flow measurements in an ESP with two-sided spike electrode [6] showed flow structures with pairs of vortices upstream and downstream from the spike electrode. These flow structures may result in a lower dust particle collection efficiency. Therefore we propose to use a discharge electrodes with spike tips on one side of the discharge electrode.

In this work we present the EHD secondary flow patterns measured in the ESP with two one-sided spike electrodes (OSSEs) directed either upstream or downstream the primary flow.

Experimental set-up

The apparatus used in this experiment for the EHD secondary flow measurements consisted of an ESP, a high-voltage supplier, and a standard PIV equipment for the measurement of velocity fields (Fig. 1).

The ESP housing used in this experiment was a transparent acrylic box, 1600 mm long, 200 mm wide and 100 mm high. At the top and bottom of the ESP two collecting stainless-steel plate electrodes (200 mm × 1100 mm) were placed. In the middle of the ESP two OSSEs with 12 spike tips each were mounted in the acrylic side-walls. Each OSSE was 200 mm long, 1 mm thick, 25 mm wide, and 15 mm tip-to-tip distance (Fig. 2). The spike tips were set parallel to the plate electrodes and transversely to the primary flow direction. The discharge electrodes were mounted so that the spikes were directed either upstream or downstream the primary flow direction. The distance from the OSSEs to the plate electrodes was 50 mm. A flow homogenizer was placed at the ESP inlet.

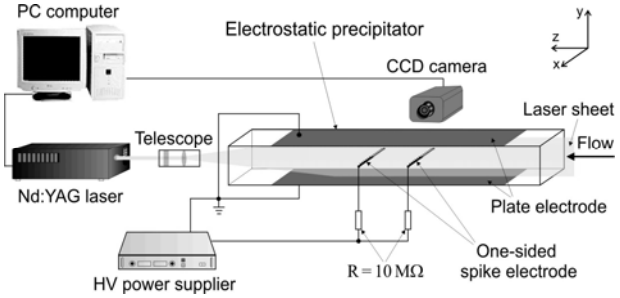

Fig. 1. Experimental set-up for PIV flow velocity field measurements in the ESP

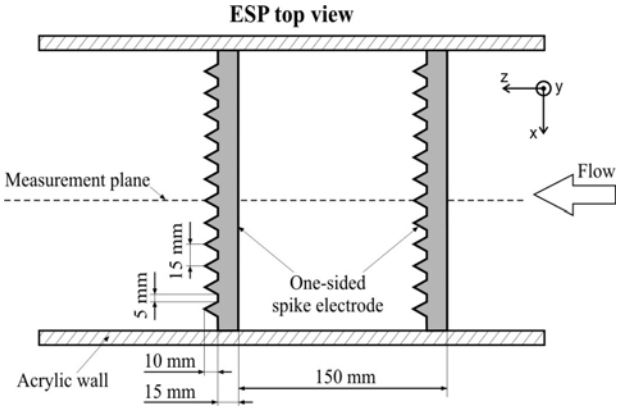

Fig. 2. Top-view schematic drawing of the ESP with OSSEs directed downstream

The air flow seeded with cigarette smoke particles was blown along the ESP duct with an average velocity of 0.9 m/s. The high voltage was supplied to the OSSEs through a 10 MΩ resistors. The negative DC voltage applied to the OSSEs was up to 27.5 kV and the total discharge current was up to 340 μA.

The EHD secondary flow measurements were carried out using Particle Image Velocimetry (PIV) equipment [7]. The PIV measurements were carried out in the cross sectional plane placed along the ESP duct, perpendicularly

to the plate electrodes (Fig. 2). The measurement plane passed through the central tips of the OSSEs, i.e. far from the acrylic side walls. A 100 instantaneous flow velocity fields were measured, then averaged and presented in this paper, what means that presented velocity maps are time-averaged.

Results

The flow velocity field measurements were carried out in the ESP at a primary flow average velocity of 0.9 m/s. At this velocity the Reynolds number was $Re = V \times L / \nu = 5700$ (the parameters used to calculate Re were: the primary flow velocity V = 0.9 m/s, characteristic length (plate-plate distance) L = 0.1 m, and air kinematic viscosity $\nu = 1.57 \times 10^{-5}$ m^2/s).

When no voltage was applied, the flow measured in the ESP was laminar (Fig. 3), corresponding to the transition region at Re > 2300.

When a high voltage was applied, the electric force exerted by the corona discharge induces a considerable EHD flow which altered significantly the primary flow. The flow patterns in the ESP changed significantly. Figures 4 to 7 show results for applied voltages of 20 kV and 27.5 kV. The time averaged discharge current was 135 μA and 340 μA, respectively. Thus the EHD numbers $[Ehd = I \times L^3 / (\nu^2 \times \rho \times \mu_j \times A)]$ [8], based on the flow channel data, were $4 \cdot 10^7$ and $1 \cdot 10^8$. Hence, the ratios of the EHD number to the Reynolds number squared (Ehd/Re^2 describes the ratio of the electric forces to the inertial force) were 1.2 (for 20 kV) and 3.1 (for 27.5 kV).

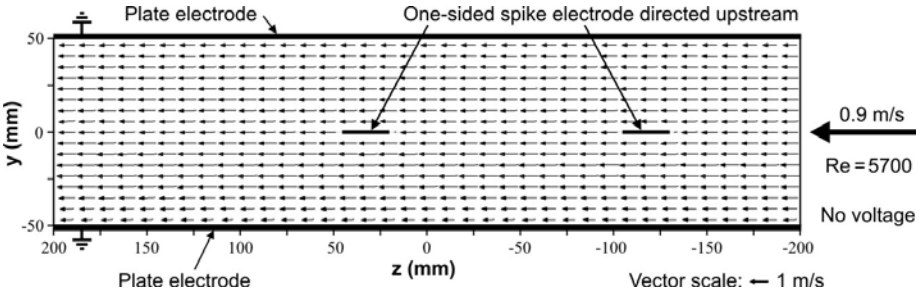

Fig. 3. Averaged flow velocity field measured in the ESP with OSSEs directed upstream the primary flow when no voltage was applied.

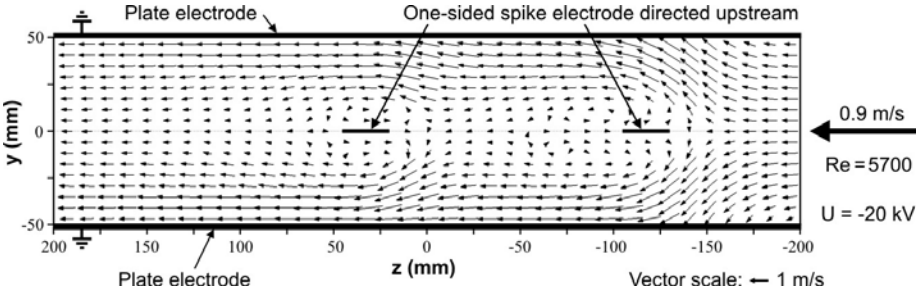

Fig. 4. Averaged flow velocity field measured in the ESP with OSSEs directed upstream the primary flow. Negative voltage of 20 kV was applied, discharge current was 135 μA.

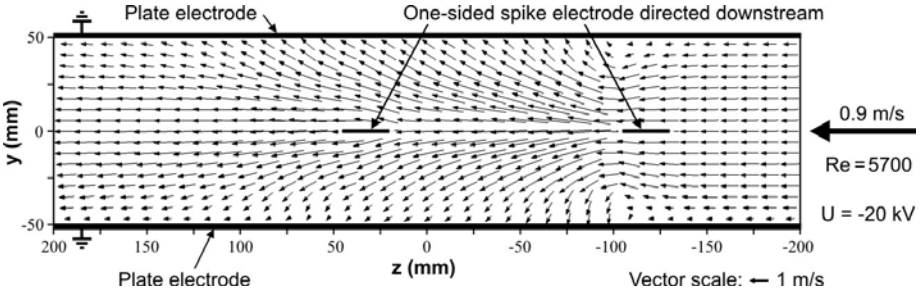

Fig. 5. Averaged flow velocity field measured in the ESP with OSSEs directed downstream the primary flow. Negative voltage of 20 kV was applied, discharge current was 135 μA.

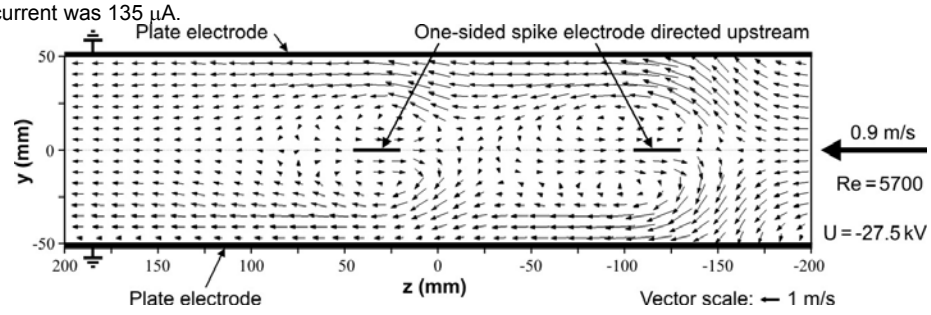

Fig. 6. Averaged flow velocity field measured in the ESP with OSSEs directed upstream the primary flow. Negative voltage of 27.5 kV was applied, discharge current was 340 μA.

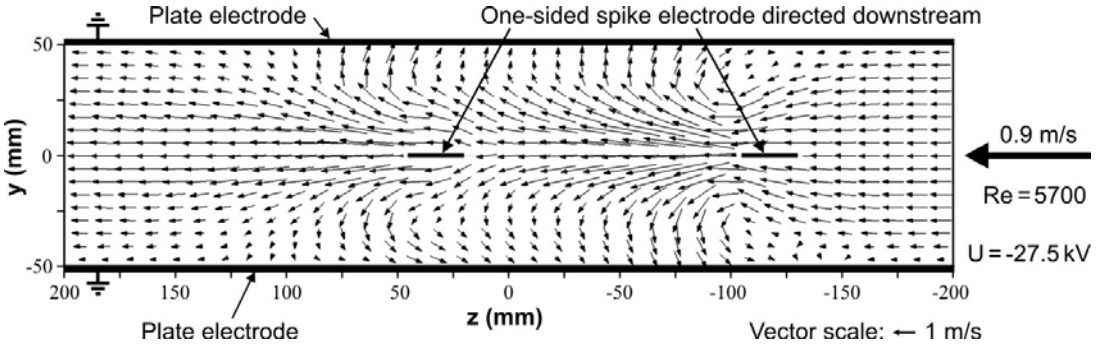

Fig. 7. Averaged flow velocity field measured in the ESP with OSSEs directed downstream the primary flow. Negative voltage of 27.5 kV was applied, discharge current was 340 μA.

The parameters used to calculate Ehd were: the total discharge current I, characteristic length (plate-plate distance) L = 0.1 m, air kinematic viscosity $\nu = 1.57 \times 10^{-5}$ m^2/s, air density $\rho = 1.205$ kg/m^3, ion mobility $\mu_i = 2.7 \times 10^{-4}$ m^2/Vs, and the discharge area (70 mm wide and 200 mm long discharge area on the two plate electrodes for the two OSSEs) A = 70 mm × 200 mm × 2 × 2 = 0.056 m^2.

Figures 4 and 5 show the averaged flow velocity fields measured for a negative applied voltage of 20 kV. Figure 4 shows results when the spike tips of the OSSEs were directed upstream the primary flow. At such position, the discharge from the spike tips generated a jet-like flow directed upstream the primary flow. It blocked the dusty air flow in the centre of the ESP duct and caused it to move nearer both plate electrodes. When the spike tips of the OSSEs were directed downstream the primary flow (Fig. 5) the downstream-directed jet-like flow behind the spike tips was observed. This jet flow caused the dusty air flow mainly along the centre of the ESP duct, at a distance from the collecting plate electrodes.

The averaged flow velocity fields in the ESP when a higher voltage of 27.5 kV was applied to the OSSEs are presented in Figures 6 and 7. The electrohydrodynamically generated flow was stronger (Ehd/Re^2 = 3.1, so the electric force dominates over the inertial one) than those observed for the lower voltage. For the upstream-directed spike tips (Fig. 6) the jet-like flow became much stronger causing a strong sucking. In consequence, a vortices were formed near the OSSEs. They caused the flow of dusty air close to the collecting plate electrodes. For the downstream-directed spike tips (Fig. 7) the jet-like flow caused the dusty air to move along the centre of the ESP duct and vortices were formed near the collecting plate electrodes (clearly seen at z position about -110 mm). These vortices block the flow along the collecting plate electrodes.

Summary

In this paper the results of the EHD secondary flow measurements in the ESP with two OSSEs are presented. The obtained results clearly show that the EHD secondary flow pattern in the ESP strongly depends on the spike tips direction and, in consequence, on the direction of the EHD flow in respect to the primary flow. For the upstream-directed spike tips the dusty air is blocked in the centre of the ESP duct and flows along collecting electrodes. For the downstream-directed spike tips the dusty air is blocked near the collecting electrodes and flows mainly through the centre of the ESP duct. The flow pattern obtained for the upstream-directed spike tips locks to be beneficial from the ESP collection efficiency point of view. To confirm better collection efficiency in the ESP with upstream-directed spike tips further investigations are needed.

Acknowledgments

The research presented in this paper received funding from the Ministry of Science and Higher Education (grant PB 327/T02/2010/70)

REFERENCES

[1] M. Mohr, S. Ylatalo, N. Klippel, E.I. Kauppinen, O. Riccius and H. Burtscher, "Submicron fly ash penetration through electrostatic precipitators at two coal power plants", Aerosol Sci. Technol., Vol. 24, pp. 191-204, 1996.

[2] S.H. Kim and K.W. Lee, "Experimental study of electrostatic precipitator performance and comparison with existing theoretical prediction models", J. Electrostat., Vol. 48, pp. 3-25, 1999.

[3] U. Kogelschatz, W. Egli and E.A. Gerteisen, "Advanced computational tools for electrostatic precipitators", ABB Review, Vol. 4, pp. 33-42, 1999.

[4] A. Mizuno, "Electrostatic precipitation", IEEE Trans. Dielectr. Electr. Insul., Vol. 7, pp. 615-624, 2000.

[5] European Parliament, Council, "Directive 2008/50/EC of the European Parliament and of the council of 21 May 2008 on ambient air quality and cleaner air for Europe", Official Journal of the European Union, L 152, 11.6.2008.

[6] J. Podliński, A. Niewulis and J. Mizeraczyk, "Electrohydrodynamic flow and particle collection efficiency of a spike-plate type electrostatic precipitator", J. Electrostat., Vol. 67, pp. 99-104, 2009.

[7] M. Raffel, Ch.E. Willert and J. Kompenhans, *Particle Image Velocimetry, A practical guide*, Springer-Verlag Berlin Heidelberg, 2007.

[8] IEEE-DEIS-EHD Technical Committee, Recommended international standard for dimensionless parameters used in electrohydrodynamics, IEEE Trans. Diel. Electr. Insul. 10-1, pp. 3-6, 2003.

***Authors**: Dr. Janusz Podliński janusz@imp.gda.pl, M.Sc. Artur Berendt aberendt@imp.gda.pl and M.Sc. Anna Niewulis aniewulis@imp.gda.pl, Centre for Plasma and Laser Engineering, The Szewalski Institute of Fluid Flow Machinery, Polish Academy of Sciences, Fiszera 14, 80-952 Gdańsk; Prof. Jerzy Mizeraczyk jmiz@imp.gda.pl, Centre for Plasma and Laser Engineering, The Szewalski Institute of Fluid Flow Machinery, Polish Academy of Sciences, Fiszera 14, 80-952 Gdańsk and Department of Marine Electronics, Gdynia Maritime University, Morska 81-87, 81-225 Gdynia*